PERGAMON

Acta mater. Vol. 47, No. 11, pp. 3263–3269, 1999

Printed in Great Britain
PII: S1359-6454(99)00179-2
1359-6454/99 $20.00 + 0.00

STRENGTHENING EFFECT OF UNSHEARABLE PARTICLES OF FINITE SIZE: A COMPUTER EXPERIMENTAL STUDY

A. W. ZHU and E. A. STARKE JR†

Department of Materials Science and Engineering, University of Virginia, Charlottesville, VA 22903, U.S.A.

(Received 19 February 1999; accepted 22 May 1999)

Abstract—Equilibrium configurations of a dislocation interacting with randomly distributed unshearable obstacles of finite size under an applied stress are analyzed. Ashby's critical dipole spacing Q' argument for the self-stress effect of dislocations is utilized but analysis suggests that the spacing Q' varies with the local obstacle distribution as well as with the obstacle shape. Computer simulations of a dislocation slip process through circular or linear obstacles, that are extensions of earlier work by Forman *et al.*, were conducted. The dependence of the strengthening stress on the obstacle size was found to be less than that predicted by equations currently in use, particularly for linear obstacles. New, modified Orowan equations are suggested for the strengthening effects due to spherical, rod-like, and plate-like obstacles. The effect of the orientation distribution of the linear obstacles demonstrated in the simulation is in agreement with recent experimental observations. © *1999 Acta Metallurgica Inc. Published by Elsevier Science Ltd. All rights reserved.*

Keywords: Aluminum; Microstructure; Dislocations; Yield phenomena; Plastic deformation

1. INTRODUCTION

The contribution of unshearable particles to the strength of alloys has been evaluated in terms of the original or modified Orowan equations [1, 2]. The original Orowan mechanism is based on an assumption that the obstacles, formed by non-shearable particles, to dislocation motion are sufficiently localized in the slip plane that they can be represented by a distribution of point forces (cf., e.g. Ref. [3]). A widely accepted equation has been derived for the increment in the critical resolved shear stress associated with the particles, i.e. "strengthening stress τ_p", as [4]

$$\tau_p = \xi \frac{Gb}{2\pi L_{cc}} \ln \frac{\chi}{r_0} \tag{1}$$

where L_{cc} denotes the planar (center-to-center) spacing between obstacles in the slip plane, G the shear modulus, and b the magnitude of the Burgers vector. r_0 and χ are the inner and the outer cut-off radius for the calculation of the dislocation line tension and parameter ξ is related to the initial dislocation character. For dislocations of the edge type or of the screw type $\xi = 1$ or $1/(1-\nu)$, respectively, where ν is Poisson's ratio.

In practical alloys, particles, e.g. precipitates, have a finite size when compared with their planar spacing in the slip plane; and they also may have a non-spherical or non-equiaxed shape. The critical stable configuration of a bowed-out dislocation segment that is pinned by two particles at two ends, and consequently the associated strengthening stress, depends on the end-to-end inter-particle spacing L_f. Therefore, an intuitive correction for the finite-size effect can simply be made by replacing L_{cc} by this effective or free spacing L_f in equation (1) (cf., e.g. Ref. [5]). For circular obstacles formed by either spherical particles or rod-like ones in a slip plane, $L_f = L_{cc} - D$ where D is the diameter of the obstacles. To calculate L_f for linear obstacles formed by plate-like particles in a slip plane, Bush and Kelly [6] considered a regular square array of parallel line segments. Kelly [7] later also used a triangular array of parallel line segments. The calculation by Nie *et al.* [8] was based on the regular "closed" triangular array of line segments. These corrections can simply be summarized as

$$\tau_p = \tau_I/(1 - \beta P/L_{cc}) \tag{2}$$

where P denotes the dimension of the obstacles (such as the diameter D of the circular ones or the length L of the linear ones) and β is a parameter that depends on the orientation of the obstacles [for instance, for (111)- or (100)-plates, $\beta = \cos(30^\circ)$]. The term τ_I includes some adjustable parameters, and can be set equal to $(\xi \cdot Gb/2\pi L_{cc})\ln(\chi/r_0)$ where a geometric mean value of $\xi = 1/(1-\nu)^{1/2}$ is often used for a general case [9, 10].

†To whom all correspondence should be addressed.

These "intuitive" treatments essentially ignored the complex statistical aspect of the geometrical configurations (position and orientation) of obstacles interacting with dislocations as well as changes due to the finite size and the specific shape of the obstacles. Melander [11] demonstrated theoretically that one effect of the finite size of circular obstacles is to change the stable configurations of the bowed-out dislocations under an applied stress, which may result in a strengthening stress LESS than that due to point-like obstacles. A computer simulation by Forman *et al*. [10] indicated that for an array of parallel linear obstacles perpendicular to the slip direction, the strengthening stress may be of the form

$$\tau_p = \tau_{II} \cdot (1 + P/L_{cc}) \tag{3}$$

where τ_{II} is the corresponding strengthening stress for point obstacles, i.e. $\tau_{II} = 0.81Gb/L_{cc}$ if the simple evaluation of the dislocation line tension $T_L = 1/2Gb^2$ is employed.

The self-stress effect of a bowed-out dislocation under an applied stress may be incorporated in τ_I in equation (2), and perhaps also in τ_{II} in equation (3). A conventional correction for this is to simply set the outer cut-off radius χ in equation (1) equal to the critical dipole spacing Q' of the face-to-face parts of the bowed-out dislocation segments, rather than to the free spacing L_f for the τ_p calculation [4, 12]. A reasonable evaluation of Q' for randomly distributed obstacles, especially of non-equiaxed shape, is still problematical. Either the length or the width of the linear obstacles formed by the plate-like particles has been somewhat arbitrarily used (e.g. Refs [7, 8, 13]).

In this work, we analyze equilibrium configurations of a dislocation interacting with randomly distributed obstacles of finite size under an applied stress. Computer experiments based on the analysis are conducted to examine the statistical aspects and to extend Forman *et al*.'s simulation of the dislocation slip process in various, and more general, cases. New modified Orowan equations are, accordingly, suggested for the strengthening effects of various particles.

2. DISLOCATION SLIP AND COMPUTER SIMULATION PROCEDURE

We will consider the interaction between a dislocation and randomly distributed obstacles in a slip plane. The obstacles are of finite size and are unshearable. For simplicity we assume, similar to the treatment in Ref. [11], that there is no stable position for the dislocation inside the obstacles. Figure 1 illustrates the "local" interaction configuration of the dislocation and the circular obstacles of (a) a regular square distribution and (b) a random distribution.

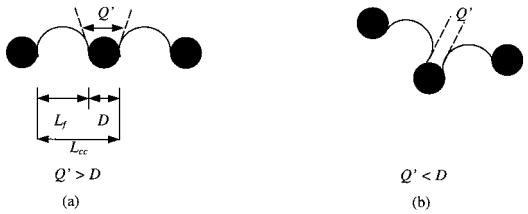

Fig. 1. Schematic illustration of the basic geometry of interaction of dislocation with unshearable obstacles of (a) a regular distribution and (b) a random distribution.

Under the action of an applied resolved shear stress τ, the dislocation is bowed out between the adjacent obstacles, tending to bypass between them and hence to slip in one slip plane and along one slip direction, e.g. (111)[$\underline{1}$10] in aluminum. The line tension of the dislocation depends on the free spacing L_f as

$$T_L = \zeta \frac{Gb^2}{4\pi} \ln \frac{L_f}{r_0}$$

where ζ is a parameter related to the dislocation character [12]. The curvature radius ρ of the dislocation line segments is $\rho = T_L/\tau b$. A larger applied stress causes the dislocation segments to be more bowed-out, and therefore spacing η between any two face-to-face bowed-out dislocation segments becomes smaller as illustrated in Fig. 2. When the two dislocation segments are close to each other within a certain critical spacing η_c, i.e. $\eta \leq \eta_c$, they annihilate and the obstacle or obstacles between them are looped away. The critical unstable local configuration of the dislocation under the applied stress will therefore depend on the curvature of the bowed-out dislocation segments and the critical spa-

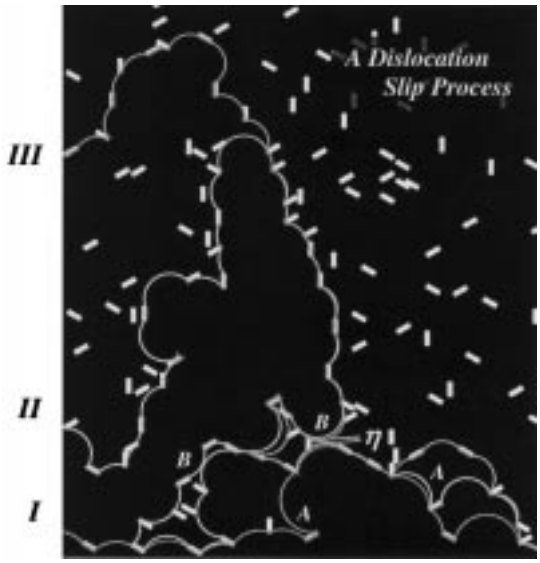

Fig. 2. Equilibrium configurations of a dislocation interacting with randomly distributed rectangular obstacles under increased applied stress (I⟹II⟹III)—part of computer simulation area. "η" denotes spacing between any two face-to-face bowed-out dislocation segments.

cing η_c that is related to the interaction between different parts (the two face-to-face bowed-out segments) of the dislocation.

A simple instability criterion $\eta = \eta_c = 0$ for any two face-to-face dislocation segments has been employed if the self elastic interaction of the dislocation is neglected [14]. In fact, the attractive interaction of any two face-to-face parts of the bowed-out dislocation segments will make it easier for dislocations to break away from the obstacle or the obstacles between the two segments. Therefore, the critical spacing η_c has to be greater than zero.

A strict treatment of the self-interaction effect under general conditions seems formidable. For an approximation, resorting to an analogous treatment as in Ref. [3], it may be assumed that the effect is accounted for by introduction of an *apparent* applied stress τ^* while the simple instability criterion is retained

$$\eta = \eta_c = 0. \tag{4}$$

In order that equation (1) with $\chi = Q'$ can simply be retrieved in our simulation when point obstacles are considered, the apparent applied stress may be written as

$$\tau^* = \tau \frac{\ln(L_f/r_0)}{\ln(Q'/r_0)} \tag{5}$$

and the corresponding apparent curvature radius of the dislocation segments therefore becomes

$$\rho^* = \frac{2T_L}{\tau^* b} = \frac{Gb}{4\pi\tau} \ln \frac{Q'}{r_0} \tag{6}$$

where we have assumed for simplicity that the parameters ξ and ζ are equal. The critical spacing Q' was considered to be larger than the dimension of the obstacles [15], and could be $4D$ for circular ones [3]. The evaluation of Q' will be discussed in detail later.

Wherever the local configuration of the dislocation becomes unstable, i.e. $\eta = \eta_c = 0$, the dislocation moves forward, bypassing those obstacle(s) until it is impeded by the next obstacle(s) resulting in a new stable configuration. A macro-slip process of the dislocation is achieved through successive "annihilation" of the local dislocation parts; pairs of face-to-face parts of the bowed-out dislocation segments. A dislocation slip process through the obstacles can be numerically simulated based on this analysis.

A structure of obstacles on a slip plane can be constructed with a random position distribution, an orientation distribution and with no overlapping (those closer than $0.1L_{cc}$ to other obstacles are excluded). A linear obstacle may be considered to be a row of closely spaced point obstacles. Similarly, rectangular obstacles and circular ones can be represented by a row of closely spaced linear obstacles, each of which, in turn, is represented by point obstacles. For instance, a rectangular obstacle of length L and width W can be represented totally by a number $(W/\lambda) \times (L/\lambda)$ of point ones with the spacing λ. The spacing $\lambda \leq 0.1L_{cc}$ is employed in the following treatment. In this way, a dislocation slip process through obstacles of any shape can be accounted for by considering the interaction of the dislocation with the corresponding closely spaced point obstacles.

Equation (6) is employed to calculate the curvature of the dislocation segments under an applied stress. The dislocation equilibrium configurations among the obstacles of certain shape in the slip plane can be figured out by means of a modified version of Morris *et al.*'s circle rolling method [16, 17] with the η-criterion [equation (4)]. The yield stress (or the particle strengthening stress τ_p) is defined as the stress at which the dislocation finds a way to slip out of a large array of obstacles. Figure 2 illustrates a dislocation slip process through a random distribution of rectangular obstacles oriented at -30, 30 and 90° with regard to the slip direction on a slip plane under an increasing applied stress.

3. COMPUTER SIMULATION RESULTS

3.1. Linear obstacles

Since plate-like particles such as the θ''-phase in Al–Cu and T_1-phase in Al–Cu–Li alloys, have large diameter-to-thickness aspect ratios (>10), they may be regarded as linear obstacles to dislocations in a slip plane. We consider 8100 obstacles with equal probability being oriented at -30, 30 and 90° with regard to the dislocation slip direction (three-variant condition). They are distributed at random on a slip plane in a square area of $90L_{cc} \times 90L_{cc}$. An image boundary condition is applied. The equilibrium configurations of a dislocation under an increased stress τ in units of $[(Gb/2\pi L_{cc})\ln(Q'/r_0)]$ is determined for the array of linear obstacles of length (L/L_{cc}). The strengthening stress τ_p in units of $[(Gb/2\pi L_{cc})\ln(Q'/r_0)]$ can thus be obtained for the obstacle structure by the simulation. The results are depicted in Fig. 3. By means of the two-order polynomial formula $[y = 0.82 \times (1 + Ax + Bx^2)]$ regression analysis where $x = L/L_{cc}$ and $y = (Gb/2\pi L_{cc})\ln(Q'/r_0)$, as shown in Fig. 3, the parameters A and B are obtained as

$$A = 0.93 \pm 0.08,\ B = 0.21 \pm 0.05. \tag{7a}$$

The corresponding results for obstacles of only 90° orientation (one-variant condition) and of only $\pm 30^\circ$ orientations (two-variant condition) are also obtained and are shown in Fig. 3. The parameters A and B by the regression analysis are

$$A = 0.94 \pm 0.10,\ B = 0.10 \pm 0.03 \tag{7b}$$

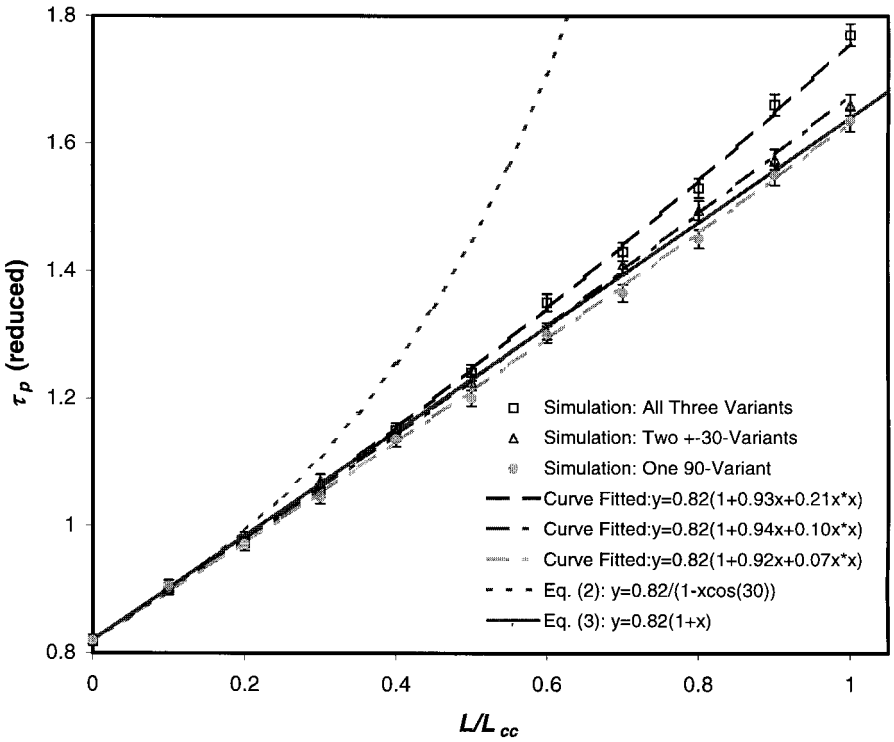

Fig. 3. Dependence of the reduced strengthening stress on the length (L/L_{cc}) of the linear obstacles.

for the case of only two $\pm 30^\circ$ variants and

$$A = 0.92 \pm 0.08, \; B = 0.07 \pm 0.03 \qquad (7c)$$

for only one 90° variant. The results in Fig. 3 indicate that there is not much difference in τ_p for the three orientation distribution conditions when $L/L_{cc} < 0.5$ but the differences increase for larger values of L/L_{cc}. The largest τ_p is achieved when the obstacles are randomly oriented (namely, all the three variants of the obstacles are present) and τ_p is slightly larger in the case of two variants of obstacles than in the one-variant case.

For the sake of comparison with respect to equations (2) and (3), the terms τ_I and τ_{II} are set equal to $(Gb/2\pi L_{cc})\ln(Q'/r_0)$. The strengthening stress predicted by equations (2) and (3) are depicted in Fig. 3 with (τ_p/τ_I) and (τ_p/τ_{II}) plotted against L/L_{cc}. It is indicated that the strengthening stress τ_p obtained in the present simulation for the one-variant condition is "nominally" close to those in the earlier computer experiments by Forman *et al.* [10]. On the other hand, the τ_p-values obtained for all the three orientation distribution conditions are evidently lower than the corresponding values according to equation (2) when $L_p/L_{cc} > 0.3$: larger differences appear at larger values of L/L_{cc}.

3.2. Circular obstacles

A similar calculation was conducted with 2500 obstacles of circular shape of diameter D. They were distributed at random in a slip plane in a square area of $50L_{cc} \times 50L_{cc}$. The results are plotted in Fig. 4 with the reduced strengthening stress $\tau_p/((Gb/2\pi L_{cc})\ln(Q'/r_0))$ plotted against D/L_{cc}. By means of regression analysis, as shown in Fig. 4, the results obtained fit well to the equation

$$\tau_p = \frac{0.82Gb}{2\pi L_{cc}} \ln \frac{D}{r_0} \left[1 + 0.83 \frac{D}{L_{cc}} + 1.91 \left(\frac{D}{L_{cc}} \right)^2 \right]. \qquad (8)$$

For comparison, the results according to equations (2) and (3) are also depicted in Fig. 4 with (τ_p/τ_I) and (τ_p/τ_{II}) plotted against D/L_{cc}.

It is evident that the dependence of τ_p on the size of the obstacles as demonstrated in the simulation is positive, opposite to Melander's conclusion [11], almost the same as that predicted by equation (2) if the other adjustable terms are equally adopted. Significant difference appears only at large values of D/L_{cc} (> 0.4).

4. DISCUSSION

In the simulation we have introduced the η-criterion to determine the instability of the dislocation configuration in terms of the spacing η of any two face-to-face bowed-out dislocation segments. Compared with the criterion in terms of the inclination angle φ between the neighboring dislocation segments on the opposite sides of one obstacle (e.g. Refs [3–5]), the η-criterion can be regarded as a general extension, particularly for *randomly* distributed *unshearable* particles of *finite size*. The η-criterion takes any two face-to-face dislocation segments into account while the φ-criterion con-

siders only the very local (neighboring) situation. As shown in the simulation, e.g. location "A" in Fig. 2, the annihilation of the two bowed-out dislocation segments separated by more than one particle is a very frequent situation.

As mentioned above, for circular obstacles having the regular distribution shown in Fig. 1(a), the value of the critical dipole spacing Q' was considered to be larger than the diameter D [15]. However, considering randomly distributed circular obstacles, the annihilation of the face-to-face parts of the two bowed-out dislocation segments will be easier for the dislocation configuration shown in Fig. 1(b). In this case, the critical spacing Q' will be somewhat less than D. Since the macro-slip process of dislocation slip is initiated and realized through the easiest micro-slip (or local movement) of dislocations, it is reasonable to use a mean value by setting $Q' = D$, rather than $> D$. In addition to this effect of the local distribution of the obstacles, evaluation of Q' also depends upon the shape of the obstacles. In the case of non-equiaxed obstacles, e.g. ones of rectangular shape as schematically shown in Fig. 5, the value of Q' could be varied between the length L and the width W, depending on the local configuration of the dislocation. For simplicity, a geometric mean value $\bar{Q} = \sqrt{(L \cdot W)}$ may be adopted for rectangular obstacles and $0.1L$ for linear obstacles.

The strengthening stress obtained for linear obstacles particularly under the one-variant condition in the present simulation is "nominally" close to those obtained in Forman *et al.*'s work where only a simple line tension argument (leading to $\tau_{II} = 0.81Gb/L_{cc}$) is applied [10]. The similarity comes from the simplification we made for incorporation of the effect for our simulation as shown in equations (5) and (6). The minor difference can be ascribed to the somewhat different circle rolling methods employed. Also, the number of obstacles considered and hence the calculation accuracy may be different. Distinct from this one-variant condition when the linear obstacles are oriented parallel, a higher strengthening stress appears particularly at the large values of (L/L_{cc}) for the three-variant condition when the obstacles are randomly oriented. This may possibly be attributed to different randomness of spatial distribution of obstacles under different orientation-distribution conditions.

Compared with the conventional "intuitive" description which leads to the currently used Orowan equations like equation (2), a less positive dependence of the strengthening stress on the dimension of obstacles (cf. Figs 3 and 4), especially in the case of linear obstacles, has been found in the simulation. This might also be a reflection of the complex statistical aspect of the interaction

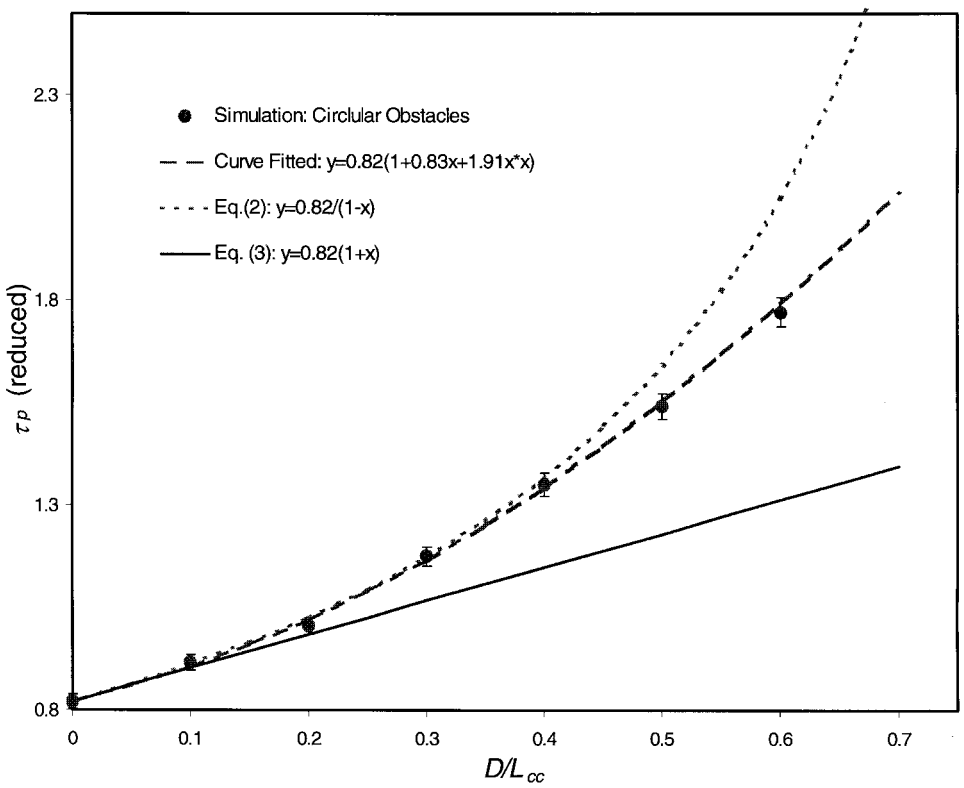

Fig. 4. Dependence of the reduced strengthening stress on the diameter (D/L_{cc}) of the circular obstacles.

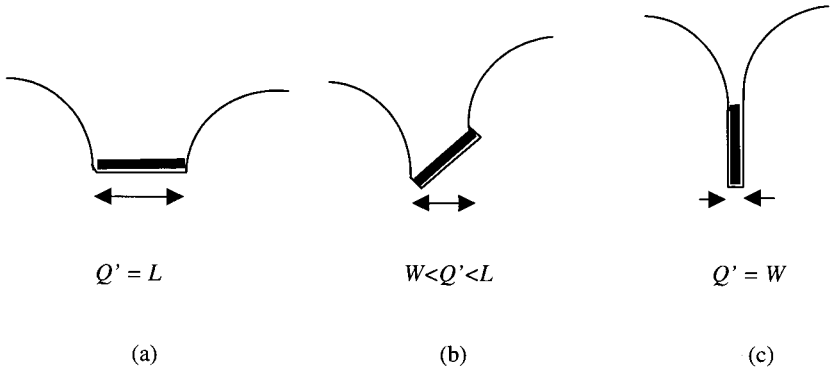

Fig. 5. Schematic illustration of the basic geometry of interaction of dislocation with a rectangular obstacle.

between dislocations and randomly distributed obstacles of finite size, which was once considered to cause even a negative dependence of τ_p on the size of circular obstacles [11]. For circular obstacles, since the typical value of (D/L_{cc}) in practical spherical particle hardened alloys is hardly >0.15 [15, 18], no difference is expected between the results of our simulation and the prediction by equations like equation (2) when compared to the relevant experimental observations [15, 18]. As for linear obstacles, values of (L/L_{cc}) are often larger than 0.5 in plate hardened alloys [1, 2]. The existing data in the literature are either scattered [12] or lack very detailed microstructural information [13]. We need direct and more systematic experimental tests and quantitative microstructural analysis of samples containing unshearable plates of size and volume fraction varied over a wide range. However, our recent work on a number of high strength aluminum alloys [14] indirectly support the simulation results.

The orientation distribution of plate-like particles or the linear obstacles in the slip plane has been shown to slightly affect the strengthening stress in the simulation. The randomly oriented obstacles cause a higher strengthening stress than the non-randomly oriented ones. This is in agreement with recent experimental observations in an Al–4Cu (Zr) alloy and a commercial Al–Cu–Mg (designated as C415) [19]. The experiments showed that a random distribution of plate-like precipitates on {100} and {111} planes, produced by conventional aging, resulted in a higher strength than aligned {100} and {111} plate precipitates (with one variant defaulted) produced by stress aging. The strength of the conventionally aged material was usually higher, but never less, than the stress-aged material regardless of the loading direction. This phenomenon is just contrary to the prediction [20] that was derived according to the continuum mechanics models which were based on deformation compatibility requirements between matrix and plate particles [21, 22]. Further work examining this phenomenon is under way.

5. CONCLUSIONS

Equilibrium configurations of a dislocation interacting with random distributed unshearable obstacles of finite size under an applied stress are analyzed and a new η-criterion of instability is introduced. Ashby's dipole spacing argument for the self-stress effect of dislocations is utilized but it is suggested that the spacing Q' varies with the local obstacle distribution as well as with the obstacle shape. The computer simulations, based on the analysis and some "isotropic assumptions", of a dislocation slip process were conducted. The dependence of the strengthening stress on the obstacle size is shown to be positive but less than those accounted for in the currently used "intuitive" Orowan equations like equation (2), especially for linear obstacles. The following modified Orowan equations are suggested.

I. For circular obstacles in a slip plane

$$\tau_p = \frac{0.82Gb}{2\pi L_{cc}} \ln \frac{D}{r_0} \left[1 + 0.83 \frac{D}{L_{cc}} + 1.91 \left(\frac{D}{L_{cc}} \right)^2 \right]:$$

For application to spherical particles of diameter D_s and volume fraction f_v, set $D = \pi/4 D_s$ and $L_{cc} = (\pi/6f)^{1/2} D_s$ [5], which yields

$$\tau_p = 0.18G \frac{b}{D_s} (f_v^{1/2} + 0.90 f_v + 2.25 f_v^{3/2}) \ln \frac{0.79 D_s}{r_0},$$

for spherical particles.

For application to ⟨100⟩ oriented rod-like particles of diameter D_r, length l_r ($\gg D_r$) and volume fraction f_v, set $D = D_r/(\cos 54.7°)^{1/2}$ and $L_{cc} = D_r(\pi/4 f_v \cos 54.7°)^{1/2}$ [23], which yields

$$\tau_p = 0.15G \frac{b}{D_r} (f_v^{1/2} + 1.84 f_v + 1.84 f_v^{3/2}) \ln \frac{1.316 D_r}{r_0},$$

for $<100>$ rod-like\ particles.

II. For linear obstacles of random orientations (i.e. all three variants are present) in the slip

plane

$$\tau_p = \frac{0.82Gb}{2\pi L_{cc}}\left[1 + 0.93\frac{L}{L_{cc}} + 0.21\left(\frac{L}{L_{cc}}\right)^2\right]\ln\frac{0.1L}{r_0}:$$

For application to {100}-plates of diameter D_p and thickness t_p ($\ll D_p$), set $L = \pi/4D_p$ and $L_{cc} = (\pi D_p t_p/4f_v \sin 54.7^\circ)^{1/2}$ [23], which yields

$$\tau_p = 0.13G\frac{b}{(D_p t_p)^{1/2}}[f_v^{1/2} + 0.75(D_p/t_p)^{1/2}f_v + 0.14(D_p/t_p)f_v^{3/2}]\ln\frac{0.079D_p}{r_0},$$

for {100} plate-like particles.

For application to {111}-plates, set $L = \pi/4D_p$ and $L_{cc} = (\pi D_p t_p/3f_v \sin 70.5^\circ)^{1/2}$ [23], which yields

$$\tau_p = 0.12D\frac{b}{(D_p t_p)^{1/2}}[f_v^{1/2} + 0.70(D_p/t_p)^{1/2}f_v + 0.12(D_p/t_p)f^{3/2}]\ln\frac{0.079D_p}{r_0},$$

for {111\} plate-like particles.

The orientation distribution of the linear obstacles is found to affect the strengthening stress, particularly at large values of (L/L_{cc}), which is qualitatively in agreement with recent experimental observations.

Acknowledgements—The authors would like to thank the office of the Naval Research for support under contract ONR N00014-91-J-1285, George Yoder, contractor monitor.

REFERENCES

1. Gilmore, D.L. and Starke, E.A. Jr, *Metall. Mater. Trans.*, 1997, **28A**, 1399.
2. Lloyd, D. J., in *ICSMA*, Vol. 3, 1985, p. 1745.
3. Kocks, U.F., *Mater. Sci. Engng*, 1977, **27**, 191.
4. Ashby, M.F., *Acta metall.*, 1966, **14**, 679.
5. Ardell, A.J., *Metall. Trans.*, 1985, **16A**, 2131.
6. Bush, M.E. and Kelly, P.M., *Acta metall.*, 1970, **19**, 1363.
7. Kelly, P.M., *Scripta metall.*, 1972, **6**, 647.
8. Nie, J.F., Muddle, B.C. and Polmear, I.J., *Mater. Sci. Forum*, 1996, **217-222**, 1257.
9. Hirsch, P. B. and Humphreys, F. J., *Physics of Strength and Plasticity*. MIT Press, Cambridge, MA, 1969, p. 189.
10. Foreman, A. J. E., Hirsch, P. B. and Humphreys, F. J., *Fundamental Aspects of Dislocation Theory*, NBS Spec. Pub. 317, Vol. 2, 1970, p. 1083.
11. Melander, A., *Physica status solidi (a)*, 1977, **43**, 223.
12. Brown, L. M. and Ham, R. K., *Strengthening Methods in Crystals*, ed. A. Kelly and R. B. Nicholson. Halsted Press, John Wiley, New York, 1971, p. 9.
13. Merler, P., Fouquet, F. and Merlin, J., *Mater. Sci. Engng*, 1981, **50**, 215.
14. Zhu, A. W., Csontos, A. and Starke Jr, E. A., *Acta mater.*, 1999, **47**, 1713.
15. Ashby, M. F., *Physics of Strength and Plasticity*. MIT Press, Cambridge, MA, 1969, p. 113.
16. Hanson, K. and Morris, J.W. Jr, *J. appl. Phys.*, 1975, **46**, 983.
17. Morris, J.W. and Klahn, D.H. Jr, *J. appl. Phys.*, 1974, **45**, 2027.
18. Hanson, N., *Acta metall.*, 1970, **18**, 137.
19. Hargarter, H., Little, M.T. and Starke, E.A. Jr, *Mater. Sci. Engng*, 1998, **257**, 87.
20. Little, M. T., Ph.D. dissertation, University of Virginia, 1996.
21. Hosford, W.F. and Zeisloft, R.H., *Metall. Trans.*, 1972, **3**, 113.
22. Bate, P., Roberts, W.T. and Wilson, D.V., *Acta metall.*, 1981, **29**, 1797.
23. Fullman, R.L., *Trans. Am. Inst. Min. Engrs*, 1953, **197**, 447.